Proceedings of the ASME 2015 34th International Conference on Ocean, Offshore and Arctic Engineering
OMAE2015
May 31-June 5, 2015, St. John's, Newfoundland, Canada

OMAE2015-41802

SHIP ROLL BEHAVIOUR IN LARGE AMPLITUDE BEAM WAVES

Jiaming Liang
School of Naval Architecture, Ocean and Civil Engineering, Shanghai Jiao Tong University
Shanghai 200240, China

Zhiliang Lin[1]
State Key Lab of Ocean Engineering, School of Naval Architecture, Ocean and Civil Engineering, Shanghai Jiao Tong University
Shanghai 200240, China

ABSTRACT

In this paper, the Homotopy Analysis Method (HAM) is applied to obtain high accuracy series solutions of roll motions of a ship, which encounters a nonlinear wave of large amplitude. Comparisons are made between roll responses in linear and nonlinear beam waves with identical wave slope and frequency. Furthermore, Floquet theory is applied to analyze the stability of HAM series solutions. Besides that, numerical simulation is used to verify the analytical solution and study the behaviors of the system under disturbance. All the results demonstrate that the proposed scheme is an effective analytic technique to study nonlinear ship rolling equation, and the stability analysis reveals the significance of researching ship roll motion in large amplitude nonlinear wave.

NOMENCLATURE

ϕ	roll angle
$\dot{\phi}$	angle velocity
$\ddot{\phi}$	angle acceleration
ϕ_a	roll response amplitude
I_{xx}	mass moment of inertia
δI_{xx}	added mass moment of inertia
$\mathrm{D}(\dot{\phi},\phi)$	nonlinear damping moment
$\mathrm{R}(\phi)$	nonlinear restoring moment
$\mathrm{M}(t)$	exciting moment
ω	frequency of encounter
ω_0	natural frequency of the motion
T_ϕ	natural period of the motion
D_1	linear damping term
D_3	nonlinear damping term
K_3, K_5	nonlinear restoring term
$\tilde{d}_1$	nondimensional linear damping term
$\tilde{d}_3$	nondimensional nonlinear damping term
$\tilde{k}_3, \tilde{k}_5$	nondimensional nonlinear restoring term
λ	nondimensional inertia term
Δ	displacement
GM	metacentric height
L_w	wavelength
H	wave height
k	wave number
A	wave amplitude

INTRODUCTION

Among the six degrees of ship motion, roll motion plays the most significant role as far as ship stability is considered. Most of the unexplained accidents and casualties at sea may be attributed to the loss of stability due to roll motion, especially its nonlinearity [1]. For this reason, it is of the utmost importance to study the mechanism of roll motion, predict roll response and evaluate the stability of roll motion in inclement environmental conditions.

Over the years, ship roll motion in beam seas has attracted considerable attention. Nayfeh and Sanchez applied Floquet theory and concepts of bifurcation theory in the analysis of the stability of ship roll motions [2]. Lin and Yim [3] developed a stochastic analysis procedure by a generalized Melnikov method to examine the properties of chaotic roll motion and capsizing of ships subjected to periodic excitation with a random noise disturbance. McCue and Troesch used Lyapunov exponents to predict chaotic vessel motions and indicated specific regions of questionable stability [4].

[1] Corresponding author. Email: linzhiliang@sjtu.edu.cn

Copyright © 2015 by ASME

The nonlinear ship roll system is represented using a mathematical model with cubic damping, and cubic and quintic restoring terms. Approximate analytical and numerical solutions have been found to describe the physical phenomenon and many methods were developed [5], such as multiple time scales method [6] and time averaging method [7]. In this paper, Homotopy Analysis Method (HAM) is applied to obtain high accuracy series solution, which differs from perturbation method in the independence of any parameter assumptions [8]. HAM is an approximate analytic method to solve strong nonlinear differential equations, originally proposed by Prof. Liao in 1992 [9]. HAM provides great freedom to choose base functions and linear auxiliary operators together with an effective way to ensure high accuracy and fast convergence of the series solution, thus it has been widely used to solve nonlinear problems in science and engineering.

Most of the previous work discussed about the encountering wave based on the linear wave theory which cannot correctly describe large beam waves. In this study, ship roll motion subjected to a nonlinear wave of large amplitude whose higher-order harmonic terms are not omitted is considered. Roll responses subjected to linear and nonlinear beam waves with same wave slope and frequency are compared. Moreover, to analyze the stability of nonlinear ship roll motion subjected to linear and nonlinear beam waves, Floquet theory [10] is applied. Besides that, a Simulink model was developed to verify the HAM series solutions and their stability.

SHIP ROLLING IN BEAM SEAS

When considering roll motions in beam seas, it is possible to ignore the coupling of rolling and other degrees of freedom of ship motion. Ship roll motions in beam waves can be modeled as the motion of a simple pendulum and the general equation reads

$$\left(I_{xx}+\delta I_{xx}\right)\ddot{\phi}+D(\dot{\phi},\phi)+R(\phi)=M(t) \tag{1}$$

If the natural frequency of the roll motion, ω_0 is known, the value of the moment of inertia is determined in the form

$$\left(I_{xx}+\delta I_{xx}\right)=\omega_0^2\Delta GM \tag{2}$$

Assuming the ship is symmetric and in upright position, the restoring moment is a function of the underwater form of the ship hull and may be approximated by a quintic polynomial of the form

$$R(\phi)=\Delta GM\,\phi+K_3\phi^3+K_5\phi^5 \tag{3}$$

The damping moment could be represented in several ways, in this work the formulation of the cubic polynomial are used

$$D(\dot{\phi},\phi)=D_1\dot{\phi}+D_3\dot{\phi}^3 \tag{4}$$

Besides that, assuming that the wavelength is large compared with the ship beam and the heading angle of the beam wave is 90 degrees, the wave exciting moment could be approximated by

$$M(t)=-I_{xx}\ddot{\alpha}(t) \tag{5}$$

NONLINEAR LARGE WAVE LOAD

For a monochromatic gravity wave with a small wave slope, according to the linear wave theory, the elevation of the free surface can be expressed as

$$\eta(x,t)=A\cos(kx-\omega t) \tag{6}$$

Thus, the local wave slope in Eqn. (5) takes the form of

$$\alpha(t)=kA\cos(\omega t) \tag{7}$$

Here, the effect of the initial phase of the encountered wave is neglected, which only represents a phase shift of the responding oscillation of the ship in a monochromatic gravity wave. Thus the exciting moment of the outer wave is written as

$$M(t)=I_{xx}kA\omega^2\cos(\omega t) \tag{8}$$

However, for a large amplitude monochromatic wave, Eqn. (6) based on the linear wave theory cannot correctly describe the free surface elevation. According to the previous work by Liao [11], the exact solution of nonlinear large amplitude wave is expressed as

$$\eta(x,t)=\sum_{n=0}^{+\infty}a_n\cos n(kx-\omega t) \tag{9}$$

where a_n represents the wave amplitude of the n-**th** wave component. Consequently, for a ship that encounters a large monochromatic wave, the local wave slope in Eqn. (5) can be described as

Copyright © 2015 by ASME

$$\alpha(t) = k\sum_{n=0}^{+\infty} a_n \cos n\omega t \tag{10}$$

Therefore, the exciting moment is written as

$$M(t) = I_{xx} k\omega^2 \sum_{n=1}^{+\infty} n^2 a_n \cos(n\omega t) \tag{11}$$

NONDIMENSIONAL SHIP ROLLING MODEL

Dividing Eqn. (1) by $(I_{xx} + \delta I_{xx})$, it is obtained that

$$\ddot{\phi} + d_1\dot{\phi} + d_3\dot{\phi}^3 + \omega_0^2\phi + k_3\phi^3 + k_5\phi^5 = \sum_{n=1}^{+\infty} F_n \cos(n\omega t) \tag{12}$$

where k_i are the relative restoring coefficients, d_i are the relative damping coefficients, $F_n = \lambda k\omega^2 n^2 a_n$ are the relative amplitudes of exciting moment, and $\lambda = I_{xx}/(I_{xx} + \delta I_{xx})$ is non-dimensional inertia term.

Furthermore, by introducing the transformation $\tau = \omega_0 t$, the new form of Eqn. (12) yields

$$\ddot{\phi} + \tilde{d}_1\dot{\phi} + \tilde{d}_3\dot{\phi}^3 + \phi + \tilde{k}_3\phi^3 + \tilde{k}_5\phi^5 = \sum_{n=1}^{+\infty} \tilde{F}_n \cos n\tilde{\omega}\tau \tag{13}$$

where $\tilde{d}_1 = d_1/\omega_0$, $\tilde{d}_3 = \omega_0 d_3$, $\tilde{k}_3 = k_3/\omega_0^2$, $\tilde{k}_5 = k_5/\omega_0^2$, $\tilde{F}_n = F_n/\omega_0^2$ and $\tilde{\omega} = \omega/\omega_0$. Therefore, the property of the nonlinear system is determined by $\tilde{d}_1$, $\tilde{d}_3$, $\tilde{k}_3$, $\tilde{k}_5$, $\tilde{F}_n$ and $\tilde{\omega}$.

HOMOTOPY ANALYSIS SCHEME

To seek the steady-state analytical solutions of Eqn. (13), the Homotopy Analysis Method is developed in this section. Firstly, defining new variable $\xi = \tilde{\omega}\tau$, Eqn. (13) becomes

$$\tilde{\omega}^2 \frac{\partial^2\phi}{\partial\xi^2} + \tilde{d}_1\tilde{\omega}\frac{\partial\phi}{\partial\xi} + \tilde{d}_3\left(\tilde{\omega}\frac{\partial\phi}{\partial\xi}\right)^3 + \phi + \tilde{k}_3\phi^3 + \tilde{k}_5\phi^5 = \sum_{n=1}^{+\infty} \tilde{F}_n \cos n\xi \tag{14}$$

The steady-state periodic solution of Eqn. (14) can be expressed as

$$\phi(\xi) = \sum_{n=0}^{+\infty} \left(a_n \sin(n\xi) + b_n \cos(n\xi)\right) \tag{15}$$

where a_n, b_n are constants to be determined.

For simplicity, define nonlinear operators as

$$\mathcal{N}[\phi] = \tilde{\omega}^2 \frac{\partial^2\phi}{\partial\xi^2} + \tilde{d}_1\tilde{\omega}\frac{\partial\phi}{\partial\xi} + \tilde{d}_3\left(\tilde{\omega}\frac{\partial\phi}{\partial\xi}\right)^3 + \phi + \tilde{k}_3\phi^3 + \tilde{k}_5\phi^5 - \sum_{n=1}^{+\infty} \tilde{F}_n \cos n\xi \tag{16}$$

Then, in the framework of HAM, the zeroth-order deformation equation is constructed as

$$(1-q)\mathcal{L}\left[\breve{\phi}(\xi;q) - \phi_0(\xi)\right] = c_0 q\mathcal{N}\left[\breve{\phi}(\xi;q)\right] \tag{17}$$

where $q \in [0,1]$ is the embedding parameter, $c_0 \neq 0$ is the convergence control parameter, $\mathcal{L}$ is the auxiliary linear operator and $\phi_0(\xi)$ is the initial estimate of $\phi(\xi)$. Obviously, there exists

$$\breve{\phi}(\xi;0) = \phi_0(\xi), \quad \breve{\phi}(\xi;1) = \phi(\xi) \tag{18}$$

That is, mapping function $\breve{\phi}(\xi;q)$ deforms from the initial estimate ϕ_0 to the exact solution ϕ as q varies from 0 to 1.

Using Taylor's theorem, $\breve{\phi}(\xi;q)$ is expanded in power series of q as follows

$$\breve{\phi}(\xi;q) = \phi_0(\xi) + \sum_{m=1}^{+\infty} \phi_m(\xi) q^m \tag{19}$$

where

$$\phi_m(\xi) = \frac{1}{m!}\frac{\partial^m \breve{\phi}(\xi;q)}{\partial q^m}\bigg|_{q=0} \tag{20}$$

Assuming that c_0 is properly chosen and the power series (19) is convergent at $q=1$, the series solution is obtained

$$\phi(\xi) = \phi_0(\xi) + \sum_{m=1}^{+\infty} \phi_m(\xi) \tag{21}$$

Copyright © 2015 by ASME

Substituting the series (19) into the zeroth-order deformation equation (17) and equating the like-power of q, the so-called mth-order deformation equation is obtained

$$\mathcal{L}\left[\phi_m(\xi)-\chi_m\phi_{m-1}(\xi)\right]=c_0R_m(\vec{\phi}_{m-1}) \tag{22}$$

where

$$\chi_m=\begin{cases}0, & m\le 1,\\ 1, & m\ge 2\end{cases} \tag{23}$$

$$\vec{\phi}_k=\{\phi_0,\phi_1,\phi_2,\cdots,\phi_k\} \tag{24}$$

and

$$\begin{aligned}R_m(\vec{\phi}_{m-1})&=\frac{1}{(m-1)!}\frac{\partial^{m-1}\mathcal{N}\left[\breve{\phi}(\xi;q)\right]}{\partial q^{m-1}}\bigg|_{q=0}\\&=(\chi_m-1)\left(\sum_{n=1}^{+\infty}\tilde{F}_n\cos n\xi\right)+\tilde{\omega}^2\frac{\partial^2\phi_{m-1}}{\partial\xi^2}+\tilde{d}_1\tilde{\omega}\frac{\partial\phi_{m-1}}{\partial\xi}\\&+\tilde{d}_3\tilde{\omega}^3\sum_{i=0}^{m-1}\sum_{j=0}^{m-1-i}\frac{\partial\phi_i}{\partial\xi}\frac{\partial\phi_j}{\partial\xi}\frac{\partial\phi_{m-1-i-j}}{\partial\xi}+\phi_{m-1}+\tilde{k}_3\sum_{i=0}^{m-1}\sum_{j=0}^{m-1-i}\phi_i\phi_j\phi_{m-1-i-j}\\&+\tilde{k}_5\sum_{i=0}^{m-1}\sum_{j=0}^{m-1-i}\sum_{k=0}^{m-1-i-k}\sum_{l=0}^{m-1-i-j-k}\phi_i\phi_j\phi_k\phi_l\phi_{m-1-i-j-k-l}\end{aligned} \tag{25}$$

Note that, the right-hand side R_m is known in the mth-order deformation equation, and the sub-problems are linear, decoupled and can be solved by means of the symbolic computation software, such as Wolfram Mathematica 9.0. The detailed solution process can be referred in Appendix A.

Consequently, at the Mth-order approximation, it exists

$$\phi(\xi)\approx\phi_0(\xi)+\sum_{m=1}^{M}\phi_m(\xi) \tag{26}$$

To demonstrate the convergence of the series solution, the discrete squared residual error is defined as

$$\mathcal{E}_n=\frac{1}{K+1}\sum_{k=0}^{K}\left(\mathcal{N}\left[\phi(\xi)\right]\big|_{\xi=k\Delta\xi}\right)^2 \tag{27}$$

where K is the number of the discrete points ($K=50$ in this paper), $\Delta\xi=\pi/K$ and $\phi(\xi)$ are the nth-order approximation of the series solution.

TEST VESSEL PARAMETERS

In order to illustrate the effectiveness of the Homotopy Analysis Method and the resulting complicated dynamics, the unbiased low freeboard model of Wright and Marshfield [6] is used in this paper. Detailed physical characteristics of the test vessel and corresponding non-dimensional parameters are listed in Tab. 1 and Tab. 2, respectively.

Table 1: COEFFICIENTS OF COSIDERED TEST VESSEL

λ	0.8
$\omega_0(rad\cdot s^{-1})$	5.278
$d_1(rad\cdot s^{-1})$	0.171
$d_3(s)$	0.108
$k_3((rad\cdot s^{-1})^2)$	-39.056
$k_5((rad\cdot s^{-1})^2)$	7.549

Table 2: CORRESPONDING NONDIMENSIONAL PARAMETERS

$\tilde{d}_1$	$\tilde{d}_3$	$\tilde{k}_3$	$\tilde{k}_5$
0.0324	0.570	-1.402	0.271

NONLINEAR BEAM WAVE INFORMATION

According to [6] the beam of the test vessel is 0.4 meter, the wave length is set as $L_w=4\text{m}$ in this paper, which is long enough compared with the vessel beam. With different wave slopes, three monochromatic gravity deep waves, which satisfy the fully nonlinear PDEs (see Liao [11]) governing the propagating deep-water wave problem, are given in the Tab. 3-5 as follows. For simplicity, only six of the main wave components in Eqn. (9) are considered.

Copyright © 2015 by ASME

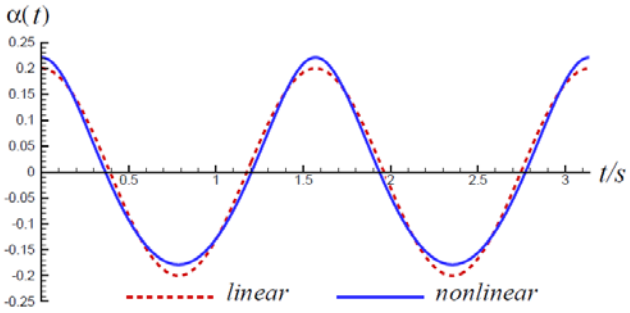

(a) CASE 1

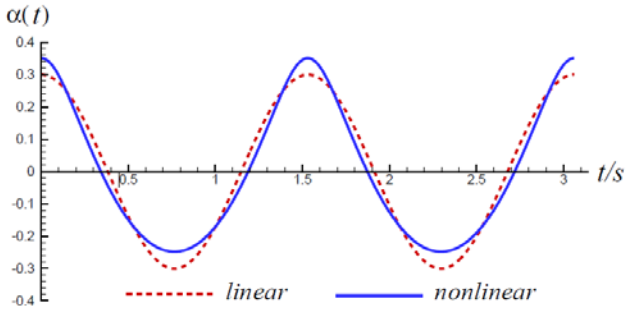

(b) CASE 2

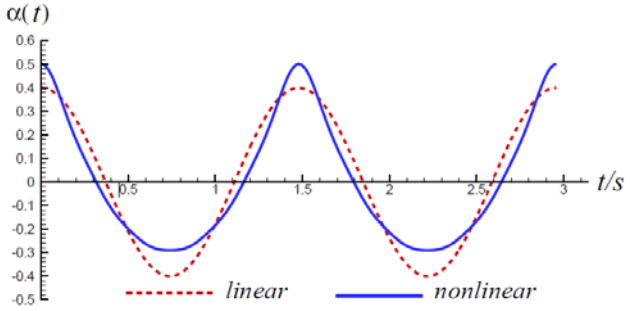

(c) CASE 3

Figure 1. LOCAL WAVE SLOPES

Table 3: BEAM WAVE INFORMATION – CASE 1

a_1	1.25164×10^{-1}	a_4	3.92717×10^{-4}
a_2	1.30581×10^{-2}	a_5	8.19823×10^{-5}
a_3	2.07357×10^{-3}	a_6	1.82049×10^{-5}
H/L_w	6.36620×10^{-2}	ω	4.00276

Table 4: BEAM WAVE INFORMATION – CASE 2

a_1	1.82295×10^{-1}	a_4	2.39072×10^{-3}
a_2	3.01474×10^{-2}	a_5	8.15455×10^{-4}
a_3	7.74436×10^{-3}	a_6	2.95614×10^{-4}
H/L_w	9.54930×10^{-2}	ω	4.10404

Table 5: BEAM WAVE INFORMATION – CASE 3

a_1	2.25563×10^{-1}	a_4	9.93992×10^{-3}
a_2	5.39358×10^{-2}	a_5	5.26656×10^{-3}
a_3	2.09279×10^{-2}	a_6	2.98442×10^{-3}
H/L_w	1.27324×10^{-1}	ω	4.24652

In order to investigate the property of ship rolling in nonlinear beam waves, the information of linear deep-water waves corresponding to foregoing three nonlinear wave cases is given below:

Table 6: LINEAR WAVE INFORMATION

	ω	L_w $(=2\pi g/\omega^2)$	H/L_w $(\times10^{-2})$	A $(\times10^{-1})$
Case 1	4.00276	3.84315	6.36620	1.22331
Case 2	4.10404	3.65580	9.54930	1.74552
Case 3	4.24652	3.41460	12.7324	2.17380

Then the local wave slopes ($\alpha(t)$, Eqns. (7) and (9)) are plotted in the Fig. 1 for different cases.

RESULTS ANALYSIS

HAM is applied to solve the rolling equation (Eqn. (12)) in six conditions, namely linear and nonlinear wave of Case 1-3, respectively. Setting $c_0 = -1$, all series solutions are expanded to 10th order with residual error less than 5×10^{-5}. Stability of the roll motion is studied in the context of Floquet theory, and details of stability analysis are stated in Appendix B. The criteria of stability is the maximum modulus of calculated eigenvalues λ_1, λ_2 of the roll motion. If $|\lambda_i|<1$, the roll motion is stable, otherwise, it is considered to be unstable.

There exist three steady-state solutions of Case 1 both in linear and nonlinear wave, two of the solutions are stable and the other is unstable, which is illustrated in Tab. 7 and shown in Fig. 2 (a). For Case 2 and 3 in both linear and nonlinear wave, there only exists one solution for each condition. The roll responses are plotted in Figure 2 (b) and (c) respectively. It is obvious that the difference between roll responses in linear and nonlinear waves becomes significant with the increment of wave slope. Especially in Case 3, there is an obvious drop of maximum roll angle from 42.8849° in linear wave to 34.6369° in nonlinear

Copyright © 2015 by ASME

wave. As shown in Tab. 8, solutions of Case 2 are both stable, but the maximum modulus of λ_i in nonlinear wave increases to 0.662, larger than that of linear wave. From Tab. 9, the maximum value of $|\lambda_i|$ is 0.243 in linear wave situation, which means that the roll response is stable, while solution in nonlinear wave is unstable since $|\lambda_i|$ reaches 1.072. Thus, in the condition of a large wave slope, the behavior of ship roll motion in nonlinear wave differs from its counterpart in linear wave.

Table 7: ROLL RESPONSE—CASE 1

		ϕ_{max}	ϕ_{min}	$\|\lambda_1\|$	$\|\lambda_2\|$
solution1	linear	38.712	-38.712	0.325	0.325
	nonlinear	39.678	-37.295	0.326	0.326
solution2	linear	14.628	-14.628	0.765	0.765
	nonlinear	12.660	-15.686	0.765	0.765
solution3	linear	29.088	-29.088	1.868	0.137
	nonlinear	29.107	-29.940	1.865	0.133

Table 8: ROLL RESPONSE—CASE 2

	ϕ_{max}	ϕ_{min}	$\|\lambda_1\|$	$\|\lambda_2\|$
linear	41.2846	-41.2846	0.276	0.276
nonlinear	39.0820	-41.0962	0.662	0.122

Table 9: ROLL RESPONSE—CASE 3

	ϕ_{max}	ϕ_{min}	$\|\lambda_1\|$	$\|\lambda_2\|$
linear	42.8849	-42.8849	0.243	0.243
nonlinear	34.6369	-43.3705	1.072	0.071

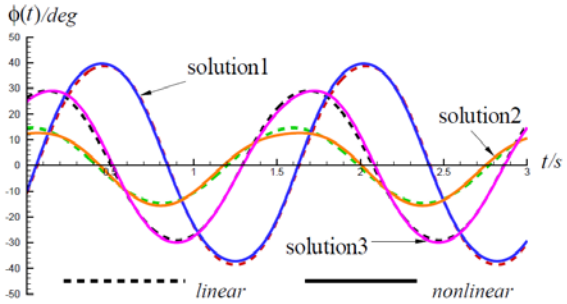

(a) CASE 1

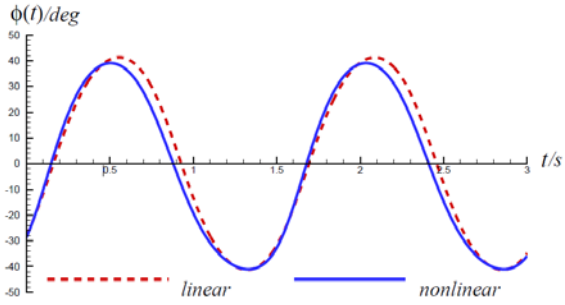

(b) CASE 2

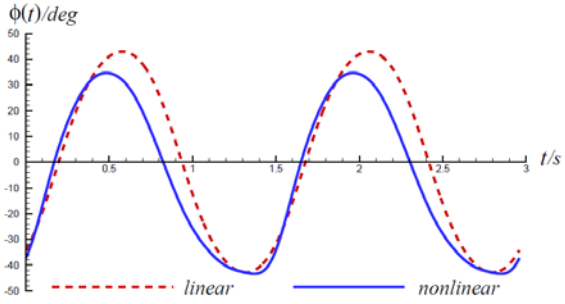

(c) CASE 3

Figure 2. ROLL RESPONSE

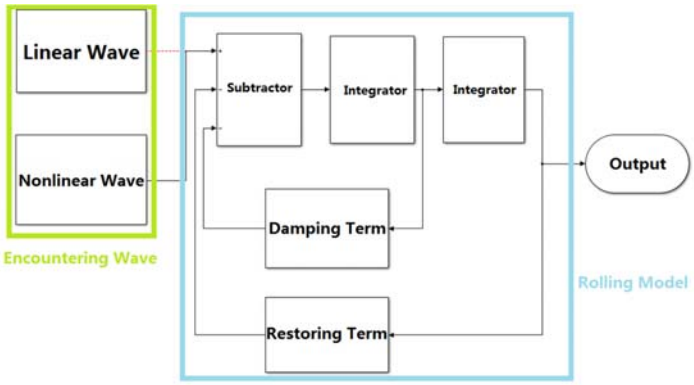

Figure 3. NUMERICAL SIMULATION

Copyright © 2015 by ASME

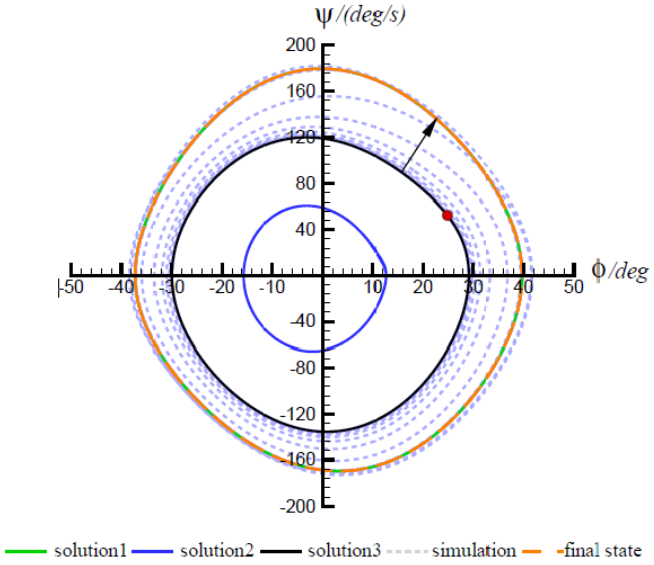

Figure 4. STABILITY ANALYSIS OF SOLUTION 3 IN CASE 1

To study the unstable solution (solution 3) in Case 1, the system is rewritten as

$$\begin{cases} \dot{\phi} = \psi \\ \dot{\psi} = -d_1\psi - d_3\psi^3 - \omega_0^2\phi - k_3\phi^3 - k_5\phi^5 - \sum_{n=1}^{+\infty} F_n \cos(n\omega t) \end{cases} \tag{28}$$

and the simulated system in Simulink is shown in Fig. 3. The "Linear Wave" and "Nonlinear Wave" blocks act as the encountering wave, also mean the exciting moment in Eqn. (12). The "Subtractor", "Integrator", "Damping Term" and "Restoring Term" blocks together act as the mathematical rolling model $\ddot{\phi} + d_1\dot{\phi} + d_3\dot{\phi}^3 + \omega_0^2\phi + k_3\phi^3 + k_5\phi^5$ in Eqn. (12). 50s roll motion is simulated with time step of 0.001s starting at the initial value of $(\phi, \dot{\phi}) = (24.82^\circ, 52.50^\circ / \mathrm{s})$, which is a point on the phase trajectory of periodic HAM series solution.

The phase trajectory of roll motion is described in Fig. 4 where the red dot represents the initial state in the numerical simulation. Three limit cycles corresponding to three steady states are also plotted in Fig. 4. In the first stage of the simulation, the phase trajectory of roll motion is close to the limit cycle of solution 3. In the progress of the simulation, the phase trajectory deviates from the limit cycle of solution 3 and tends to the limit cycle of solution 1 in the final stage. The numerical simulation demonstrates the unstable characteristics of solution 3, for the truncation error of the initial state serves as a disturbance.

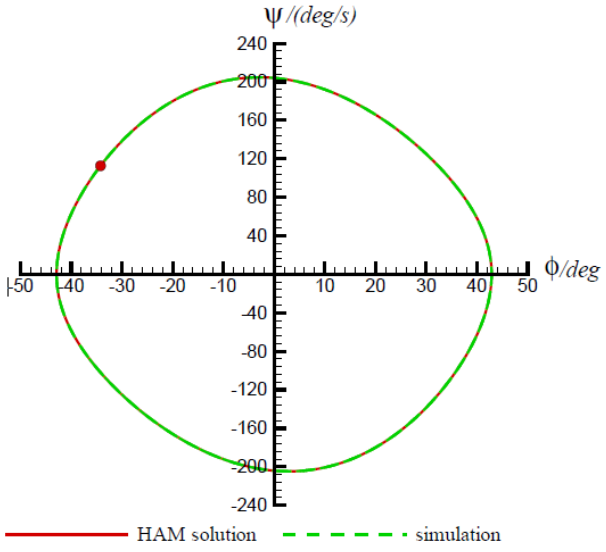

(a) LINEAR WAVE CONDITION

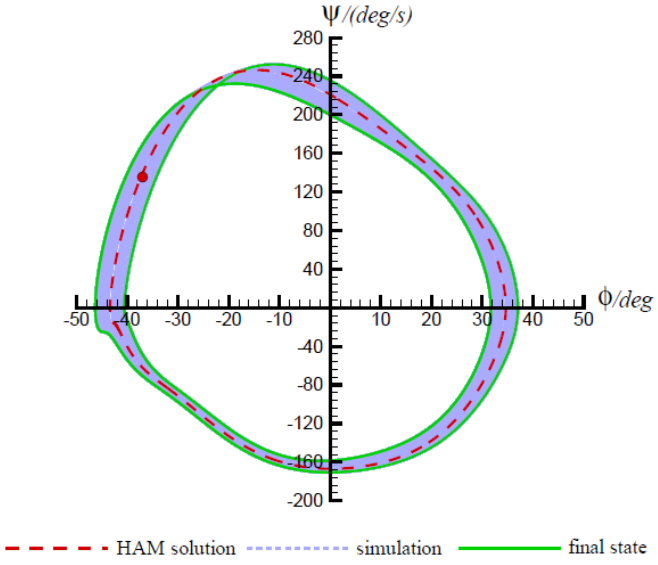

(b) NONLINEAR WAVE CONDITION

Figure 5. STABILITY ANALYSIS OF THE SOLUTION IN CASE 3

Similarly, to study the stability of the solution in Case 3, 500s roll motion is simulated with time step 0.001s, and numerical results are plotted in Fig. 5. For linear wave condition, the roll motion is stable, and the solution obtained by HAM is in high conformity with the numerical simulation as shown in Fig. 5 (a). This validates the accuracy and effectivity of HAM. For nonlinear wave condition, although there is an obvious drop of

Copyright © 2015 by ASME

maximum roll angle from the linear condition, the roll motion of HAM series solution is unstable, which is further demonstrated by the numerical simulation as shown in Fig. 5 (b). When the wave slope is large, e.g. $H / L_w = 1.27324 \times 10^{-1}$ as shown in Tab. 5, the ship roll motion in nonlinear wave is unstable, since the maximum absolute value of the eigenvalue is $|\lambda_1| = 1.072$ in Tab. 9.

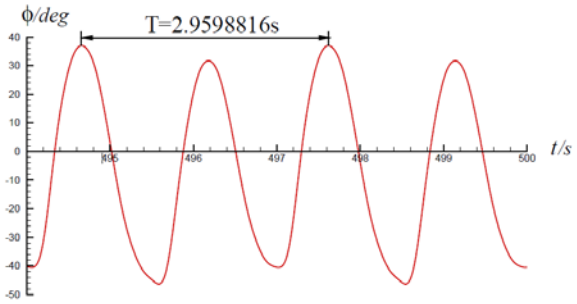

Figure 6. FINAL ROLL RESPONSE STATE IN CASE 3 BASED ON NUMERICAL SIMULATION

Due to the unstable characteristics, the ship roll motion doesn't tend to the limit cycle of the HAM solution of Case 3. According to the numerical simulation, the final state is plotted in Fig. 6. It shows that the final state is a double closed cycle with period $T = 2.9598816s$, which is almost twice of the period of encountering beam wave ($T = 2\pi / \omega = 1.4796081s$).

CONCLUSIONS

In this paper, we apply Homotopy Analysis Method to analyze ship roll behavior in large amplitude beam waves. The approximate analytical solutions of the nonlinear roll equation are obtained with high accuracy and stability of each solution is studied in the context of Floquet theory. Obvious difference between roll responses of linear and nonlinear waves are observed. The following conclusions are drawn:

1) An effective HAM scheme is successfully proposed to solve the steady states of the equation of ship roll motion in nonlinear waves, which is validated by numerical simulation.

2) In Case 1, when wave slope is small, there are three solutions of roll responses, and solutions in nonlinear wave are almost the same with their counterparts of linear wave. One of the solutions is unstable and finally shifts to one of the other two stable solutions under disturbance.

3) When the wave slope becomes larger, the difference of roll motions between linear and nonlinear encountering waves gets more significant.

4) In Case 3, when the wave slope is large enough, even if the roll amplitude in nonlinear wave is smaller than its counterpart in linear wave, the roll motion of HAM solution becomes unstable. Based on numerical simulation, the period of roll motion in nonlinear wave is almost twice of that of the encountering beam wave.

In conclusion, the results above demonstrate that the proposed Homotopy Analysis Method is an effective analytic technique to study the steady states of ship roll motion in beam waves, and the stability analysis in this paper reveals the significance of researching ship roll motion in large amplitude nonlinear waves.

ACKNOWLEDGMENTS

The authors would like to express thanks to the Natural Science Foundation of China (No. 51209136) for the finance support on this work.

REFERENCES

[1]Taylan M., 2000. The effect of nonlinear damping and restoring in ship rolling, Ocean Engineering, vol. 27(9), pp. 921 – 932.

[2]Nayfeh A. H., 1990. Sanchez N. E., Stability and complicated rolling responses of ships in regular beam seas, International shipbuilding progress, vol. 37(410), pp. 177-198.

[3]Lin H., Yim S., 1995. Chaotic roll motion and capsize of ships under periodic excitation with random noise, Applied Ocean Research, vol. 17(3), pp. 185-204.

[4]McCue L. S., Troesch A. W., 2011. Use of Lyapunov exponents to predict chaotic vessel motions, Contemporary Ideas on Ship Stability and Capsizing in Waves, Springer Netherlands, pp. 415-432.

[5]Pedišić Buča M., Senjanović I., 2006. Nonlinear ship rolling and capsizing, Brodogradnja, vol. 57(4), pp. 321-331.

[6]Right J.R.G., Marshfield W.B., 1980. Ship roll response and capsize behavior in beam seas, Trans. R. Inst. Nav. Archil., vol. 122, pp. 129-148.

[7]Wellicome, J.F., 1975. An analytical study of the mechanism of capsizing, Proc. Int. Conf. on Stability of Ships and Ocean Vehicles, Glasgow.

[8]Liao, S.J., 2003. Beyond Perturbation: Introduction to the Homotopy Analysis Method, Chapman & Hall/CRC Press, Boca Raton.

[9]Liao S.J., 1992. Proposed homotopy analysis techniques for the solution of nonlinear problem. Ph.D. thesis, Shanghai Jiao Tong University.

[10]Nayfeh, A.H., 1981. Introduction to perturbation techniques, New York, Wiley Interscience.

[11]Liao S.J., Cheung K.F., 2003. Homotopy analysis of nonlinear progressive waves in deep water, Journal of Engineering Mathematics, vol. 45(2), pp. 105–116.

Copyright © 2015 by ASME

Appendix A: HAM Solution Process

In the framework of HAM, there is a great freedom to choose the initial estimate $\phi_0(\xi)$ and the auxiliary linear operator $\mathcal{L}$. Under the rule of solution expression (15), it is straightforward to choose

$$\phi_0(\xi) = a_0 \sin\xi + b_0 \cos\xi \tag{A.1}$$

and

$$\mathcal{L}[f] = \tilde{\omega}^2[\frac{\partial^2 f}{\partial \xi^2} + f] \tag{A.2}$$

where a_0 and b_0 are constants to be determined. The auxiliary linear operator has the property

$$\mathcal{L}[C_1 \sin\xi + C_2 \cos\xi] = 0 \tag{A.3}$$

where C_1 and C_2 are constants.

Considering the rule of solution expression (15) and the property of the auxiliary linear operator $\mathcal{L}$, Eqn. (25) can be expressed as

$$R_m(\vec{\phi}_{m-1}) = a_{m,1}\sin\xi + b_{m,1}\cos\xi + \sum_{i=2}^{I_m} a_{m,i}\sin(i\xi) + \sum_{j=2}^{J_m} b_{m,j}\cos(j\xi) \tag{A.4}$$

where $a_{m,i}$, $b_{m,j}$ are coefficients. If $a_{m,i} \neq 0$ or $b_{m,j} \neq 0$, the solution of the m th-order deformation equation, Eqn. (22), contains the so-called secular term $\xi\sin\xi$ or $\xi\cos\xi$, which disobeys the rule of solution expression, Eqn. (15). To avoid this situation,

$$a_{m,1} = 0, \quad b_{m,1} = 0 \tag{A.5}$$

are enforced. Therefore, the solution of Eqn. (22) is obtained

$$\phi_m(\xi) = \chi_m\phi_{m-1}(\xi) + \sum_{i=2}^{I_m} \bar{a}_{m,i}\sin(i\xi) + \sum_{j=2}^{J_m} \bar{b}_{m,j}\cos(j\xi) + \bar{a}_{m,1}\sin\xi + \bar{b}_{m,1}\cos\xi \tag{A.6}$$

where

$$\bar{a}_{m,i} = \frac{a_{m,i}}{(1-i^2)\tilde{\omega}^2}, \quad (i = 2,\cdots,I_m) \tag{A.7}$$

$$\bar{b}_{m,j} = \frac{b_{m,j}}{(1-j^2)\tilde{\omega}^2}, \quad (j = 2,\cdots,J_m) \tag{A.8}$$

and $\bar{a}_{m,1}$, $\bar{b}_{m,1}$ are unknown coefficients which can be determined in the $(m+1)$ th-order deformation equation. Note that Eqn. (A.5) provides a set of additional algebraic equations for $\bar{a}_{m-1,1}$ and $\bar{b}_{m-1,1}$, which makes the problem closed.

Appendix B: Stability Analysis

To ascertain the stability of the roll motion, the Floquet Theory [10] is applied. Considering the infinitesimal disturbance $\varepsilon(t)$, the rolling motion is in the form

$$\bar{\phi}(t) = \phi(t) + \varepsilon(t) \tag{B.1}$$

Substituting $\bar{\phi}(t)$ into Eqn. (13) and keeping only linear terms of $\varepsilon(t)$, it follows

$$\ddot{\varepsilon} + (d_1 + 3d_3\dot{\phi}^2)\dot{\varepsilon} + (\omega_0^2 + 3k_3\phi^2 + 5k_5\phi^4)\varepsilon = 0 \tag{B.2}$$

which is a linear ordinary differential equation with periodic coefficients. Due to

$$\phi(t+T) = \phi(t) \tag{B.3}$$

Eqn. (B.2) is periodic with period T. There exist two linearly independent solutions $\varepsilon_1(t)$ and $\varepsilon_2(t)$, and the fundamental matrix solution of Eqn. (B.2) is defined as

$$\Phi(t) = \begin{pmatrix} \varepsilon_1(t) & \dot{\varepsilon}_1(t) \\ \varepsilon_2(t) & \dot{\varepsilon}_2(t) \end{pmatrix} \tag{B.4}$$

which satisfies

$$\Phi(t+T) = C \cdot \Phi(t) \tag{B.5}$$

Copyright © 2015 by ASME

where C is a monodromy matrix associated with the fundamental matrix solution $\Phi(t)$.

Introducing $\Psi(t)=\begin{pmatrix}\xi_1(t) & \dot{\xi}_1(t)\\ \xi_2(t) & \dot{\xi}_2(t)\end{pmatrix}$, there exists

$$\Phi(t)=P\cdot\Psi(t) \tag{B.6}$$

where P is a constant nonsingular matrix. Substituting Eqn. (B.6) into Eqn. (B.5), it holds

$$\Psi(t+T)=P^{-1}CP\cdot\Psi(t)=B\cdot\Psi(t) \tag{B.7}$$

where B is a diagonal matrix in the form of $B=\begin{pmatrix}\lambda_1 & 0\\ 0 & \lambda_2\end{pmatrix}$ and B and C are similar matrices. Thus,

$$\xi_1(t+T)=\lambda_1\xi_1(t),\ \ \xi_2(t+T)=\lambda_2\xi_2(t) \tag{B.8}$$

It follows from Eqn. (B.8) that

$$\xi_1(t+nT)=\lambda_1^n\xi_1(t),\ \ \xi_2(t+nT)=\lambda_2^n\xi_2(t) \tag{B.9}$$

where n is an integer. Consequently, as time evolves $(n\to\infty)$

$$\xi_i\to\begin{cases}0, & \text{if}\quad |\lambda_i|<1\\ \infty, & \text{if}\quad |\lambda_i|>1\end{cases} \tag{B.10}$$

and the disturbance $\varepsilon(t)$ becomes unbounded with time if the modulus of any eigenvalue is larger than 1.

Copyright © 2015 by ASME